# Aging Effects on Aqueous Humour Flow

Han Nee Yong
Department of Mathematical Sciences, Faculty of Science, Universiti Teknologi Malaysia

Yeou Jiann Lim
Department of Mathematical Sciences, Faculty of Science, Universiti Teknologi Malaysia

Zuhaila Ismail
Department of Mathematical Sciences, Faculty of Science, Universiti Teknologi Malaysia

https://doi.org/10.5109/7395614

出版情報：Proceedings of International Exchange and Innovation Conference on Engineering & Sciences (IEICES). 11, pp.868-873, 2025-10-30. International Exchange and Innovation Conference on Engineering & Sciences
バージョン：

# Aging Effects on Aqueous Humour Flow

Han Nee Yong[1], Yeou Jiann Lim[1], Zuhaila Ismail[1]
[1]Department of Mathematical Sciences, Faculty of Science, Universiti Teknologi Malaysia, 81310 UTM Johor,
zuhaila@utm.my

**Abstract:** *This study presents a numerical investigation of aqueous humour (AH) dynamics in the anterior chamber of the human eye, focusing on the effects of aging and posture. Unlike previous works that consider the entire eyeball, a simplified two-dimensional anterior eye model is developed while preserving key physiological characteristics. Three age-specific models are constructed, capturing anatomical changes due to aging. AH flow is modelled as buoyancy-driven by thermal gradients between the cornea and internal eye structures. The finite element method, applied through the Galerkin weighted residual approach, is used to solve the coupled flow and heat equations. Results show that aging reduces AH velocity and circulation due to narrowed geometries and decreased thermal convection. Additionally, the standing position maintains stronger flow circulation than supine position across all age groups. These findings emphasize the interplay between aging and posture in regulating intraocular fluid dynamics and may inform future diagnostic and therapeutic strategies for age-related ocular conditions.*

**Keywords:** Aqueous humour flow; anterior chamber; aging; finite element.

## 1. INTRODUCTION

The human eye relies on intricate mechanisms to maintain structural and functional integrity. The anterior chamber, located between the cornea and the iris, contains AH – a transparent fluid essential for nourishing avascular tissues such as the cornea and the lens while maintaining intraocular pressure [1]. The production, circulation, and drainage of AH are tightly regulated processes that are critical for preserving ocular health. AH is produced by the ciliary body, flows through the pupil into the anterior chamber, and exits predominantly via the trabecular meshwork and Schlemm's canal with a smaller fraction draining through the uveoscleral pathway [2]. Disruptions in this dynamic system, whether caused by aging or pathological conditions, can disturb the delicate intraocular balance and contribute to the onset of diseases such as glaucoma.

In a biological context, age has a direct physiological consequence to the human eye. Anatomical and functional changes with aging are particularly impactful, impairing the AH transport mechanism. Notably, age-related morphological changes such as reduced chamber depth and anterior displacement of the lens [3-6] have been strongly associated with angle-closure glaucoma. Decrease in anterior depth due to lens thickening and anterior displacement constrict the flow domain and alter fluid dynamics [7]. Additionally, age-related thickening and anterior positioning of the lens lead to the narrowing of the iridocorneal angle, thus blocking the drainage of AH and elevating the intraocular pressure [8]. Concurrently, the trabecular meshwork responsible for the majority of AH drainage experiences structural stiffening and reduced cellularity with age, further impeding drainage efficiency [9]. The narrowing and reduced area of Schlemm's canal with aging contributes to increased outflow resistance, exacerbating intraocular pressure elevation and disrupting the balance between inflow and outflow of AH [10, 11].

Beyond structural changes, aging also impacts the dynamic processes responsible for the AH circulation. Specifically, the older population exhibits smaller anterior chamber depth and volume, decreased aqueous flow, and diminished uveoscleral outflow compared to their younger counterparts [12]. AH production declines progressively with age, with an estimated 15-35% reduction between ages 20 to 80 [12-16]. This decline results in reduced flow velocities and less effective convection within the anterior chamber. Simultaneously, the AH drainage decreases by approximately 30% over the same age range [13, 14], primarily due to increased flow resistance in the trabecular meshwork and uveoscleral pathways. Nevertheless, intraocular pressure typically remains relatively stable throughout adulthood until the later decades of life when a gradual increase is commonly observed [17, 18].

Modelling the effects of aging on ocular structures requires an interdisciplinary approach, combining concepts from biomechanics, thermodynamics, and fluid dynamics. Over the years, computational simulations have utilized two-dimensional and three-dimensional models to investigate ocular thermodynamics and fluid dynamics within the eye [19-23]. Multiple numerical techniques including the finite element method, finite volume method, boundary element method, and Lattice Boltzmann method have been employed to account for the complexities of biological tissue properties, heat transfer, and fluid mechanics [24-28]. Despite these advances, modelling age-dependent changes in anterior ocular fluid mechanics and heat transfer remains an area requiring further investigation.

Prior research has attempted to incorporate aging effects by altering geometric parameters of the anterior chamber, modifying outflow resistance, and varying thermal properties. Papaioannou and Samaras [29] presented a model that studied ocular thermoregulation across varying age groups under different ocular geometries and tear evaporation rates. Bhandari et al. [30] extended this work by examining how aging influences AH flow and drug transport. Rahman et al. [31] introduced blood perfusion and metabolism into simulations of temperature distribution within the aging eye. Despite these contributions, few studies isolate and systematically analyze anterior chamber dynamics under aging using a coupled flow-thermal model.

This study proposes a novel, computationally efficient model of the anterior segment that investigates the effects of aging on AH flow dynamics and heat transfer in both standing and supine postures. Unlike full-eye models, the present work develops a streamlined anterior chamber model that isolates the effects of aging on AH dynamics using a coupled flow-heat approach, offering a balance between physiological relevance and computational efficiency. The finite element method, implemented through Galerkin weighted residual formulation, is employed to numerically solve the coupled fluid and thermal equations. The model captures age-related changes in anterior chamber geometry, AH inflow and outflow, trabecular meshwork properties, and ocular surface temperature. This approach systematically explores how aging and posture affect intraocular flow patterns, circulation strength, and thermal stability. The use of a reduced anterior-segment-only domain while retaining key flow characteristics is expected to provide more targeted insights into age-related ocular fluid dynamics. The result may inform early detection strategies and the development of posture-specific or age-adapted interventions for related ocular disorders.

## 2. MATHEMATICAL MODEL

In the present study, two-dimensional models of the anterior segment of the eye [see Figure 1] are designed for three age groups; young (20 – 29 years), middle-aged (40 – 49 years), and elderly (60 – 69 years), based on the dimensions shown in Table 1.

Table 1. Dimensions of the anterior chamber by age group [5, 29, 30, 32, 33]

| Age group (years) | 20-29 | 40-49 | 60-69 |
|---|---|---|---|
| Anterior chamber depth, ACD (mm) | 3.43 | 3.26 | 3.01 |
| Relative lens position, RLP (mm) | 5.39 | 5.31 | 5.28 |
| Anterior chamber radius (mm) | 6.5 | 6.4 | 6.3 |
| Trabecular meshwork length, TML (mm) | 0.6 | 0.6 | 0.6 |
| Trabecular meshwork width, TMW (mm) | 0.1 | 0.1 | 0.1 |
| Iris thickness, IT (mm) | 0.4 | 0.4 | 0.4 |

The AH is considered a viscous, Newtonian, and an incompressible fluid [34]. Navier-Stokes and heat equations in steady state are implemented to model the flow dynamics of AH and temperature variation in the AC of the eye. Referring to equations proposed in [35], the governing equations for the present study are written as in Eq. (1-4).

$$\frac{\partial u}{\partial x}+\frac{\partial v}{\partial y}=0. \tag{1}$$

$$\rho\left(u\frac{\partial u}{\partial x}+v\frac{\partial u}{\partial y}\right)+\frac{\partial p}{\partial x}-\mu\left(\frac{\partial^2 u}{\partial x^2}+\frac{\partial^2 u}{\partial y^2}\right)+\rho g\alpha(T-T_c)=0. \tag{2}$$

$$\rho\left(u\frac{\partial v}{\partial x}+v\frac{\partial v}{\partial y}\right)+\frac{\partial p}{\partial y}-\mu\left(\frac{\partial^2 v}{\partial x^2}+\frac{\partial^2 v}{\partial y^2}\right)=0. \tag{3}$$

$$k\left(\frac{\partial^2 T}{\partial x^2}+\frac{\partial^2 T}{\partial y^2}\right)-\rho c\left(u\frac{\partial T}{\partial x}+v\frac{\partial T}{\partial y}\right)=0. \tag{4}$$

where $p$ refers to the AH pressure, $u$ and $v$ are the AH velocity in the $x$ and $y$ direction respectively, while $T$ is the AH temperature. $g = 9.8\text{ms}^{-1}$ denotes the gravitational acceleration which under normal circumstances acts in the positive $x$-direction. The other parameters described in Eq. (1-4) are the AH dynamics properties obtained from literature [36, 37] and the thermal properties taken from [38]. These values are listed in Table 2.

Table 2. Values of AH and thermal properties.

| Description | Value |
|---|---|
| AH thermal expansion coefficient, $\alpha$ | $3\times10^{-4}\text{K}^{-1}$ |
| AH specific heat, $c$ | $4200\ \text{Jkg}^{-1}\text{K}^{-1}$ |
| AH thermal conductivity, $k$ | $0.57\text{Wm}^{-1}\text{K}^{-1}$ |
| AH dynamic viscosity, $\mu$ | $0.9\times10^{-3}\text{kgm}^{-3}$ |
| AH density, $\rho$ | $1000\text{kgm}^{-3}$ |
| Temperature at iris or pupil, $T_p$ | 310.15K |
| Temperature at cornea, $T_c$ | 308.15K |
| Porosity, $\varepsilon$ | 0.15 |
| Permeability, $\kappa$ | $2\times10^{-15}\text{m}^2$ |

AH secreted from the ciliary body enters the anterior chamber through the posterior chamber and pupil and leaves the anterior chamber via the trabecular meshwork and Schlemm's canal [34]. As seen in Figure 2, the conditions for the boundaries of AH flow and the temperature are expressed in Eq. (6-9) and Eq. (10-11) respectively.

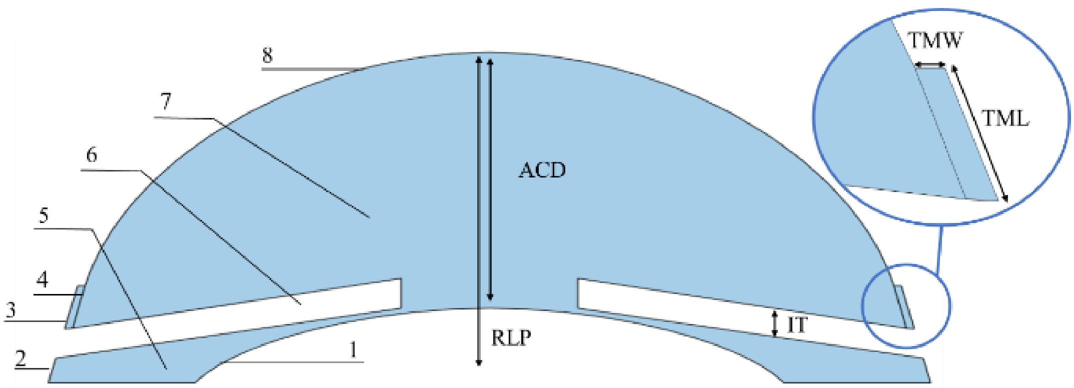


Fig. 1. Schematic diagram of the anterior segment of the eye. 1. Lens, 2. ciliary body, 3. Schlemm's canal, 4. trabecular meshwork, 5. posterior chamber, 6. iris, 7. anterior chamber, and 8. cornea.

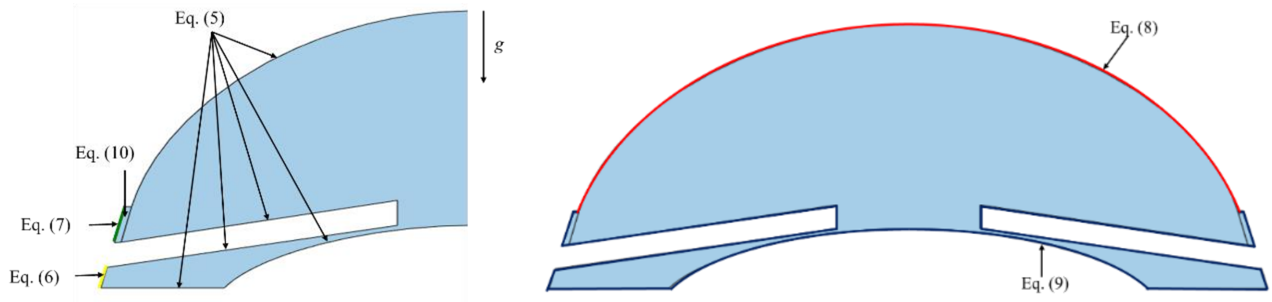

Fig. 2. Boundary conditions for AH flow and heat transfer

$$u(h(y), y) = v(h(y), y) = 0 \quad (5)$$
$$v_0 = v_{in} \quad (6)$$
$$p_0 = 1200\,Pa \quad (7)$$
$$T(g(y), y) = T_c \quad (8)$$
$$T(h(y), y) = T_p \quad (9)$$

The no-slip condition, represented as Eq. (5), is applied to all other boundaries except the inlet and outlet boundaries. Eq. (6) represents the normal inlet velocity magnitude of AH [39] where its value is different according to age group [see Table 3] while Eq. (7) describes the pressure at the outlet boundary [34]. Meanwhile, Eq. (8) is imposed on the surface of the cornea while the other boundaries are fixed with Eq. (9).

Table 3. Inlet velocity for different age groups [30]

| Age group (years) | 20-29 | 40-49 | 60-69 |
|---|---|---|---|
| Inlet velocity, $v_{in}$ ($\mathrm{ms^{-1}}$) | $2.22\times10^{-6}$ | $2.06\times10^{-6}$ | $1.90\times10^{-6}$ |

The trabecular meshwork is porous in nature, and thus the AH flow at this region is modelled through porous media. Using Stokes-Brinkman, the AH flow through the trabecular meshwork is described as Eq. (10) below [39],

$$\nabla p = -\frac{\mu}{\kappa}\boldsymbol{u} + \frac{\mu}{\varepsilon}\nabla^2\boldsymbol{u} \quad (10)$$

where κ is the permeability of trabecular meshwork and $\varepsilon$ is the porosity of trabecular meshwork [34, 39] with values as mentioned in Table 2.

### 2.1 Computational Simulation

The governing equations, Eq. (1-5), along with the prescribed boundary conditions, Eq. (6-11), are solved using the finite element method. The computational domain is discretized into non-uniform, unstructured triangular elements based on Taylor-Hood element formulation. Specifically, quadratic shape functions, $P_2$, are used for velocity and temperature, while linear shape functions, $P_1$, are employed for pressure. This $P_2 - P_1$ pairing ensures compatibility with the Ladyzhenskaya-Babuska-Brezzi condition and provides enhanced accuracy in resolving the flow and thermal gradients [40]. Within each finite element, $e_i$, the flow variables – $u$, $v$, and $p$, and temperature, $T$, are approximated using appropriate shape functions. The Galerkin weighted residual method is applied to transform the governing equations into discrete weak form. This results in a nonlinear algebraic system represented in matrix form, where the element matrices incorporate contributions from flow coupling with buoyancy-driven thermal effects. These local element matrices are assembled into a global system of equations which is then solved subject to the boundary conditions. Due to the nonlinear nature of the Navier-Stokes and heat equations, the global system is solved iteratively using the Newton-Raphson method to ensure convergence of the solution.

The numerical results are computed using the developed MATLAB code. Firstly, a mesh test is performed to ensure mesh-independent solutions. Table 4 below portrays the velocity profiles along a vertical line passing through the geometric centre of the cornea with a total number of elements 7030, 8804, 10030, 27922, and 28570. The velocity profiles are almost similar, illustrating that the results do not depend on the number of mesh elements. Hence, Mesh 3 [see Figure 3] is used to simulate the result in the present study.

Table 4. Mesh test for different total number of elements.

| Mesh | Domain element | Maximum velocity |
|---|---|---|
| 1 | 7030 | 4.5764-4 |
| 2 | 8804 | 4.4519E-4 |
| 3 | 10030 | 4.5969E-4 |
| 4 | 27922 | 4.4707E-4 |
| 5 | 28570 | 4.5474E-4 |

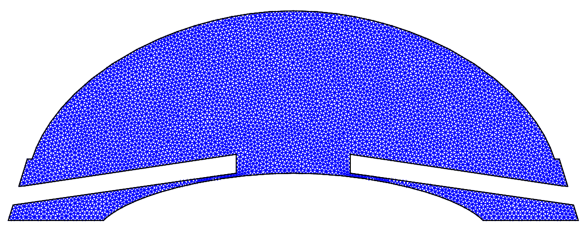

Fig. 3. Computational mesh with 10030 elements.

A comparison of the velocity magnitude in the standing and supine positions is shown in Table 5. Using the young eye model, the comparison implies that the results of the present simulation are in the order ($10^{-4}$ $\mathrm{ms^{-1}}$ and $10^{-5}$ $\mathrm{ms^{-1}}$) of the observed results in the literature. However, the differences in the maximum velocity magnitude in the anterior segment of the eye are due to the variation of the research methodologies of the different studies such as the different boundary conditions as well as the human eye model used.

Table 5. Comparison of maximum velocity magnitude of AH flow

| Eye position | Present study | Rahman et al. [31] | Jen et al. [37] |
|---|---|---|---|
| Standing | 4.60E-4 | 1.82E-4 | 2.44E-4 |
| Supine | 7.88E-5 | 7.51E-5 | 6.67E-5 |

## 3. RESULTS AND DISCUSSION

The influence of aging on AH flow dynamics is investigated by simulating three anterior eye geometries representing the young, middle-aged, and elderly configurations. These variations reflect anatomical changes typically associated with aging, such as narrowing of the anterior chamber angle and reduced anterior chamber depth.

In the young eye model (Figure 4(a)), the AH exhibited a well-organized circulation pattern characterized by a strong forward flow from the ciliary body, downward flow along the cornea, and return flow along the iris. This behaviour was maintained by the corneal thermal gradient and the chamber space, allowing efficient mixing and transport of AH within the anterior chamber of the eye. As aging progressed, the anterior chamber depth decreased, which resulted in a more confined flow domain. In the middle-aged model (Figure 4(b)), the central flow velocity diminished, and the secondary flow recirculation zones became more prominent. In the elderly model (Figure 4(c)), flow was markedly slower. These changes suggest that aging reduces the effectiveness of convective transport within the anterior chamber, potentially impairing delivery and removal of AH from the anterior segment of the eye. In addition, the elder eye shows a lower velocity magnitude, attributed to the reduced inlet velocity prescribed in the model to reflect the age-related decline in the rate of AH production.

In contrast, the supine position resulted in a shift of flow direction and weakened thermal convection due to the alignment of gravity with the inflow-outflow axis. A similar phenomenon happens in the supine positions where the velocity magnitude decreases with age. Across all age groups, velocity magnitudes are generally lower in the supine configurations compared to the standing posture. The suppression of buoyancy-driven flow is evident in the elderly eye (Figure 4(f)), where flow is the slowest. This reduction in circulation may be due to inefficient drainage of AH in aged eyes when lying down.

Overall, the results highlight that both aging and postural orientation significantly affect AH flow. Aging induces geometrical constraints that reduce velocity and circulation strength, while postural changes modulate gravitational effects on fluid dynamics. These findings align with results observed in the literature [30, 31]. The simplified anterior eye models developed in the present study thus provide a useful framework to analyse biomechanical mechanisms contributing to age-related ocular diseases.

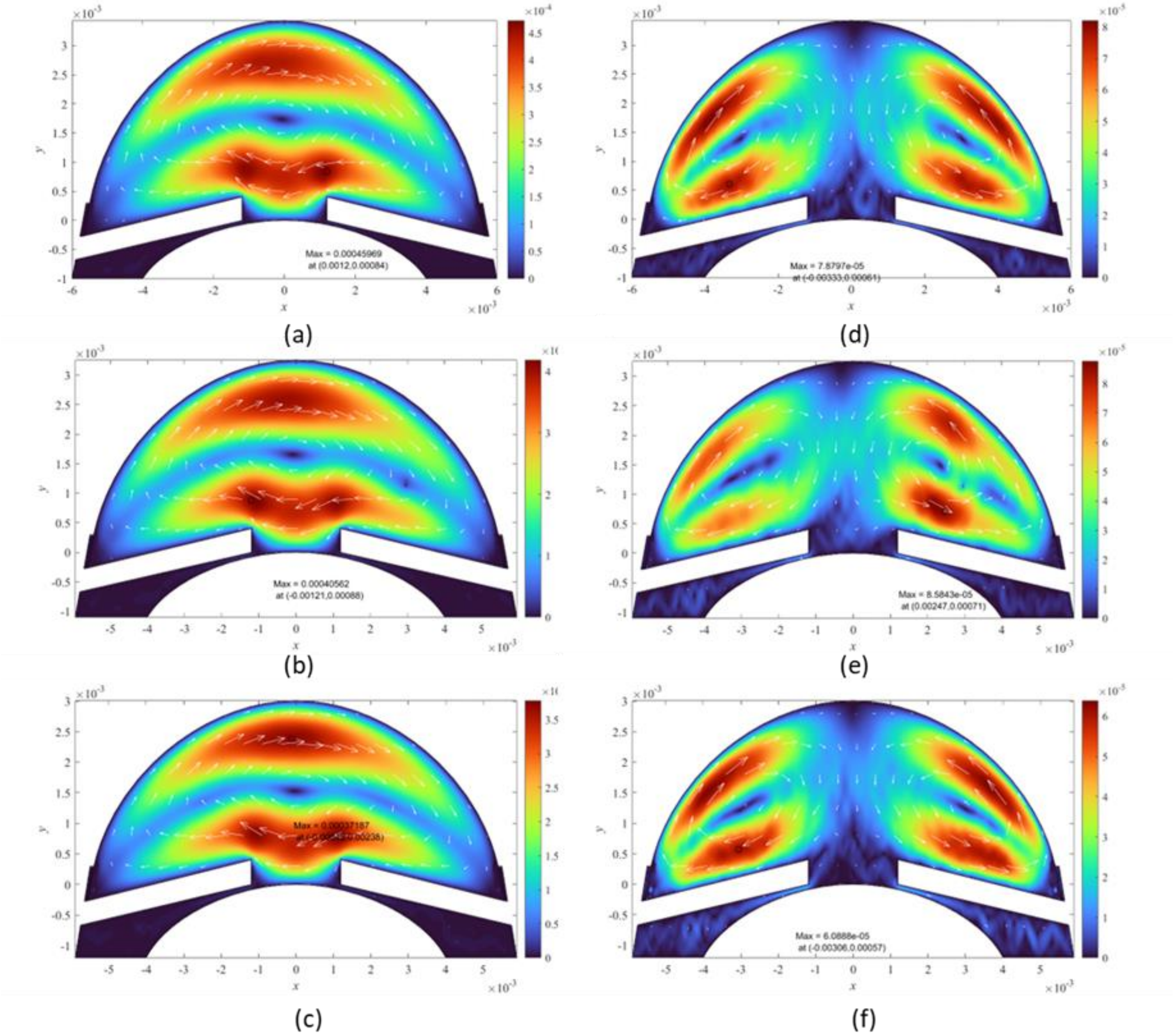


Fig. 4. AH flow in standing position for (a) young eye (20-29 years), (b) middle-age eye (40-49 years), and (c) elderly eye (60-69 years) while in supine position for (d) young eye (20-29 years), (e) middle-age eye (40-49 years), and (f) elderly eye (60-69 years).

## 4. CONCLUSION

The present study presented a simplified computational approach for analysing AH dynamics within the anterior segment of the human eye, focusing on the influence of aging. By isolating the anterior chamber and incorporating anatomical variations across different age groups, the present model successfully captures the fluid flow behaviour without the added complexity of modelling the entire eye structure. The results demonstrate that

(a) Aging significantly influences the velocity of AH flow. Reduced anterior chamber volume and narrower angles in aged eyes result in lower flow velocities and disrupted circulation.
(b) Postural changes modulate AH dynamics. The standing position promotes circulation, particularly in the younger eye whereas the supine position dampens convective effects.

Overall, the use of finite element analysis of fluid flow dynamics coupled with thermal effects and realistic boundary conditions proves effective in capturing the complex interplay between fluid flow and aging. Future extensions of the present work may include incorporating fluid-structure interaction to model eye structure deformation and more detailed physiological properties such as viscoelastic tissue responses or tear evaporation. Advanced numerical frameworks such as the coupling of Lattice Boltzmann with finite element analysis [41] as well as leverage experimental tools like 3D-printed ophthalmological examination devices [42] hold promise for simulating microscale flow interactions and bridge the gap between simulation and clinical practice.

## ACKNOWLEDGEMENT

This research was funded by the Research Management Centre (RMC), Universiti Teknologi Malaysia (UTM), Grant UTM Fundamental Research under vote number (UTMFR: Q.J130000.3854.23H02).

## REFERENCES

[1] Goel, M., R.G. Picciani, R.K. Lee, et al., Aqueous humor dynamics: a review, The Open Ophthalmology Journal, 4 (2010) 52-59.
[2] Mark, H.H., Aqueous humor dynamics and the iris, Med Hypotheses, 60 (2003) 305-8.
[3] Lowe, R.F., Anterior lens displacement with age, Br J Ophthalmol, 54 (1970) 117-21.
[4] Fontana, S.T. and R.F. Brubaker, Volume and depth of the anterior chamber in the normal aging human eye, Arch Ophthalmol, 98 (1980) 1803-8.
[5] Lim, K.J., S.M. Hyung, and D.H. Youn, Ocular dimensions with aging in normal eyes, Korean J Ophthalmol, 6 (1992) 19-31.
[6] Qin, B., X.T. Zhou, D. Huang, et al., Effects of age on ocular anterior segment dimensions measured by optical coherence tomography, Chin Med J (Engl), 124 (2011) 1829-34.
[7] Charman, W.N., The eye in focus: accommodation and presbyopia, Clin Exp Optom, 91 (2008) 207-25.
[8] Lin, J.B., K. Tsubota, and R.S. Apte, A glimpse at the aging eye, NPJ Aging Mech Dis, 2 (2016) 16003.
[9] Grossniklaus, H.E., J.M. Nickerson, H.F. Edelhauser, et al., Anatomic alterations in aging and age-related diseases of the eye, Invest Ophthalmol Vis Sci, 54 (2013) ORSF23-7.
[10] Chen, Z., J. Sun, M. Li, et al., Effect of age on the morphologies of the human Schlemm's canal and trabecular meshwork measured with swept-source optical coherence tomography, Eye (Lond), 32 (2018) 1621-1628.
[11] Li, Z., Z. Meng, W. Qu, et al., The Relationship Between Age and the Morphology of the Crystalline Lens, Ciliary Muscle, Trabecular Meshwork, and Schlemm's Canal: An in vivo Swept-Source Optical Coherence Tomography Study, Front Physiol, 12 (2021) 763736.
[12] Toris, C.B., M.E. Yablonski, Y.L. Wang, et al., Aqueous humor dynamics in the aging human eye, Am J Ophthalmol, 127 (1999) 407-12.
[13] Becker, B., The decline in aqueous secretion and outflow facility with age, Am J Ophthalmol, 46 (1958) 731-6.
[14] Gaasterland, D., C. Kupfer, R. Milton, et al., Studies of aqueous humour dynamics in man. VI. Effect of age upon parameters of intraocular pressure in normal human eyes, Exp Eye Res, 26 (1978) 651-6.
[15] Brubaker, R.F., S. Nagataki, D.J. Townsend, et al., The effect of age on aqueous humor formation in man, Ophthalmology, 88 (1981) 283-8.
[16] Gabelt, B.T. and P.L. Kaufman, Changes in aqueous humor dynamics with age and glaucoma, Prog Retin Eye Res, 24 (2005) 612-37.
[17] Klein, B.E., R. Klein, and K.L. Linton, Intraocular pressure in an American community: The Beaver Dam Eye Study., Investigative Ophthalmology & Visual Science, 33 (1992) 2224-2228.
[18] Nomura, H., F. Ando, N. Niino, et al., The relationship between age and intraocular pressure in a Japanese population: the influence of central corneal thickness, Curr Eye Res, 24 (2002) 81-5.
[19] Heys, J.J. and V.H. Barocas, A boussinesq model of natural convection in the human eye and the formation of Krukenberg's spindle, Ann Biomed Eng, 30 (2002) 392-401.
[20] Fitt, A.D. and G. Gonzalez, Fluid mechanics of the human eye: aqueous humour flow in the anterior chamber, Bull Math Biol, 68 (2006) 53-71.
[21] Ooi, E.H. and E.Y. Ng, Simulation of aqueous humor hydrodynamics in human eye heat transfer, Comput Biol Med, 38 (2008) 252-62.
[22] Karampatzakis, A. and T. Samaras, Numerical model of heat transfer in the human eye with consideration of fluid dynamics of the aqueous humour, Phys Med Biol, 55 (2010) 5653-65.
[23] Villamarin, A., S. Roy, R. Hasballa, et al., 3D simulation of the aqueous flow in the human eye, Med Eng Phys, 34 (2012) 1462-70.
[24] Ng, E.Y. and E.H. Ooi, FEM simulation of the eye structure with bio-heat analysis, Comput Methods Programs Biomed, 82 (2006) 268-76.
[25] Ooi, E.H. and E.Y.K. Ng, Effects of natural convection within the anterior chamber on the ocular heat transfer, International Journal for Numerical Methods in Biomedical Engineering, 27 (2010) 408-423.
[26] Martinez Sanchez, G.J., C. Escobar Del Pozo, J.A. Rocha Medina, et al., Numerical simulation of the aqueous humor flow in the eye drainage system; a healthy and pathological condition comparison, Med Eng Phys, 83 (2020) 82-92.

[27] Qin, Z., L. Meng, F. Yang, et al., Aqueous humor dynamics in human eye: A lattice Boltzmann study, Math Biosci Eng, 18 (2021) 5006-5028.

[28] Tang, H., Z. Qin, and B. Wen, Geometric Model and Numerical Study of Aqueous Humor Hydrodynamics in the Human Eye, Comput Math Methods Med, 2022 (2022) 4756728.

[29] Papaioannou, A. and T. Samaras, *Thermal modeling of the ageing eye*. Image Analysis and Modeling in Ophthalmology. 2014: CRC Press.

[30] Bhandari, A., A. Bansal, and N. Sinha, Effect of aging on heat transfer, fluid flow and drug transport in anterior human eye: A computational study, J Control Release, 328 (2020) 286-303.

[31] Rahman, M.A., M. Rabbani, M.H. Maruf, et al., Characterizing the Aging Process of the Human Eye: Tear Evaporation, Fluid Dynamics, Blood Flow, and Metabolism-Based Comparative Study, Biomed Res Int, 2022 (2022) 2805402.

[32] Dubbelman, M., H.A. Weeber, R.G. van der Heijde, et al., Radius and asphericity of the posterior corneal surface determined by corrected Scheimpflug photography, Acta Ophthalmol Scand, 80 (2002) 379-83.

[33] Crowder, T.R. and V.J. Ervin, Numerical simulations of fluid pressure in the human eye, Applied Mathematics and Computation, 219 (2013) 11119-11133.

[34] Ferreira, J.A., P. de Oliveira, P.M. da Silva, et al., Numerical simulation of aqueous humor flow: From healthy to pathologic situations, Applied Mathematics and Computation, 226 (2014) 777-792.

[35] Zuhaila, I., L.Y. Jiann, S. Sharidan, et al., Aqueous humour dynamics in anterior chamber under influence of cornea indentation, Fifteenth Asian Congress of Fluid Mechanics (15acfm), 822 (2017)

[36] Ismail, Z., L.Y. Jiann, S. Ahmad Jamali, et al., Simulation of AH flows and deformation of DMD in a 3D AC, Malaysian Journal of Fundamental and Applied Sciences, 13 (2017) 362-366.

[37] Jen, W.W., Z. Ismail, and A. Fitt, Simulation of Aqueous Humour Flow Driven by Buoyancy Effects and Flow Through Pupil Aperture During Descemet Membrane Detachment, CFD Letters, 12 (2020) 12-23.

[38] Ismail, Z., L.Y. Jiann, H.S. Ahmad, et al., Fluid mechanics of the descemet's membrane detachment with spontaneous reattachment., Malaysian Journal of Mathematical Sciences, 10 (2016) 19-31.

[39] Loke, C.Y., E.H. Ooi, M.S. Salahudeen, et al., Segmental aqueous humour outflow and eye orientation have strong influence on ocular drug delivery, Applied Mathematical Modelling, 57 (2018) 474-491.

[40] Reddy, J.N. and D.K. Gartling, *The Finite Element Method in Heat Transfer and Fluid Dynamics*. 3rd Edition ed. 2010.

[41] Sawayama, K., T. Tsuji, and Y. Fujimitsu, Coupling Approach of Lattice Boltzmann Fluid Simulation and Finite Element Analysis of Geophysical Properties: Application to Natural Rock Fracture in Geothermal Area, Proceedings of International Exchange and Innovation Conference on Engineering & Sciences (IEICES), 5 (2019) 73-76.

[42] Abdul Halim, A., A. Firdaus, A. Nor Azimah Abd, et al., Development of Ophthalmology Eye Examination Device Using 3D Printing Technology, Proceedings of International Exchange and Innovation Conference on Engineering & Sciences (IEICES), 10 (2024) 457-462.